

Mechanical and chemical analysis of plasma and ultraviolet–ozone surface treatments for thermal bonding of polymeric microfluidic devices†

Arpita Bhattacharyya^{*a} and Catherine M. Klapperich^{ab}

Received 24th January 2007, Accepted 27th March 2007

First published as an Advance Article on the web 27th April 2007

DOI: 10.1039/b700442g

Here we have demonstrated that radio frequency plasma and ultraviolet–ozone (UVO) surface modifications are effective treatments for enabling the thermal bonding of polymeric microfluidic chips at temperatures below the T_g (glass transition temperature) of the polymer. The effects of UVO and plasma treatments on the surface properties of a cyclic polyolefin and polystyrene were examined with X-ray photoelectron spectroscopy (XPS), contact angle measurements, atomic force microscopy (AFM) surface roughness measurements and surface adhesion measurements with AFM force–distance data. Three-point bending tests using a dynamic mechanical analyzer (DMA) were used to characterize the bond strength of thermally sealed polymer parts and the cross-sections of the bonded microchannels were evaluated with scanning electron microscopy (SEM). The experimental results demonstrated that plasma and UVO surface treatments cause changes in the chemical and physical characteristics of the polymer surfaces, resulting in a decrease in T_g at the surface, and thus allowing the microfluidic chips to be effectively bonded at temperatures lower than the T_g of the bulk polymer without losing the intended channel geometry.

Introduction

Low material cost and desirable mechanical and optical properties make engineering thermoplastics an attractive class of materials for the manufacture of disposable microfluidic devices for many applications, including capillary electrophoresis, chromatography, multianalyte immunoassays, DNA sequencing, and others.^{1–4} Due to the growing interest in disposable microfluidic devices, several plastic-chip manufacturing processes have been developed in recent years, including X-ray photolithography,⁵ hot-embossing or imprinting,^{6,7} laser ablation,⁸ injection molding,¹ *etc.* With all these methods, the fabricated substrates are sealed on the top with a cover plate of the same plastic material to form enclosed microstructures.

Sealing the channels and reagent/waste reservoirs is critical for the application of microfluidic devices. Several methods for sealing of polymeric substrates have been demonstrated, including thermal bonding in a convection oven, in water or with heated platens, PDMS films, adhesive tapes, solvent bonding, and thermal lamination.^{9–12} Of these methods, thermal bonding approaches are especially desirable since they allow the formation of a uniform channel surface comprised entirely of the same polymeric material. Other sealing approaches unavoidably introduce multiple materials to form the microchannels. This causes inhomogeneities in the ζ -potential along the channels and causes undesired effects on

the electro-hydrodynamics of the microsystems, such as Taylor dispersion and reduced electrophoretic separation efficiencies.⁹ However, conventional thermal bonding approaches still face the severe challenges of microchannel deformation, low reproducibility and poor yield, which call for continuing research to improve the thermal bonding methods.

Thermal bonding is usually performed at or near the T_g (glass transition temperature) of the polymer with the application of a small amount of pressure. Slight variance of the pressures and temperatures during the bonding process can cause deformation or complete obliteration of the microchannels at one extreme, or create a poor seal between the plastic pieces on the other. Muck *et al.* have demonstrated thermal bonding of polymethylmethacrylate (PMMA) substrates (clamped between two glass plates) at 108 °C for 10 min in a conventional oven,¹³ while Locascio *et al.* have successfully performed thermal bonding of polystyrene (PS) parts in a oven at 108 °C for 10 min by applying pressure through a clamping device.¹⁴ The bonding temperatures in both the above mentioned cases are above the T_g of the polymers (T_g of PMMA is 105 °C and that of PS is 100 °C). At these temperatures, the polymer parts are slightly deformed resulting in uneven channel walls, which can cause band broadening and affect low level detection in bioanalytical processes. Thermal bonding experiments in our laboratory with a cyclic polyolefin (Zeonor 750R, T_g 70 °C) have been done at the T_g under 500 psi for 2 min in a hot press (Heated Press 4386, Carver, Wabash, IN, USA), and for PS (Vicat softening point 93.3 °C), bonding was done at 93 °C under similar pressure and time conditions. Fig. 1 shows the cross-sections of sealed channels. As seen in the Figure, the channel walls became slightly uneven after the thermal sealing process. Attempts at thermal bonding of the polymer parts at temperatures below T_g have been

^aBiomedical Engineering, 44 Cummington Street, Boston, USA.

E-mail: abhatta@bu.edu; Fax: +1-617-353-6766; Tel: +1-617-358-3082

^bManufacturing Engineering, 44 Cummington Street, Boston, USA.

E-mail: catherin@bu.edu; Fax: +1-617-353-6766; Tel: +1-617-358-0253

† Electronic supplementary information (ESI) available: Supplementary Figures S1–S4. See DOI: 10.1039/b700442g

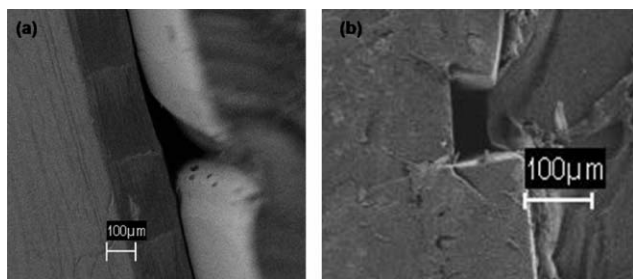


Fig. 1 Cross-sections of thermally bonded microchannels. The channels are prone to distortions during bonding. (a) Zeonor chip bonded at 70 °C, (b) PS chip bonded at 93 °C.

unsuccessful, allowing fluids to flow between channels and it is even possible to pull apart the bonded pieces with the application of a minimal amount of force. However, if the thermal bonding can be successfully done at a temperature below the T_g of the polymer, the dimensions of the channels will not be compromised. To achieve this goal, the polymer surfaces have to be modified to lower the surface T_g below the bulk T_g of the polymer.

Girault *et al.* have shown that polyethylene terephthalate (PET) substrates can be thermally sealed at temperatures substantially below the T_g of PET by surface treating both the microfabricated substrate and the cover piece with oxidative plasma.¹⁵ Truckenmüller *et al.* have shown that UV irradiation lowers the T_g of PMMA surfaces by photodegradation and allows PMMA microstructures to be welded at low temperatures.¹⁶ Activated oxygen, or ultraviolet-ozone (UVO) surface treatments are also used in industrial processes to enhance adhesion, presumably by lowering the surface T_g of the polymer. However, little published work can be found describing how the glass transition temperature of the polymer surface changes after exposure to plasma or UVO treatment. One possible explanation is that oxidative treatment produces lower molecular weight fragments on the surface through chain scission and oxidative reaction, resulting in lower T_g at the surface layer. Callan *et al.* have demonstrated that UVO treatment of polystyrene surfaces produce oxidized polymer surfaces comprising of C—O, C=O, and O—C=O type groups.¹⁷ Lubarsky *et al.* have shown through XPS (X-ray photoelectron spectroscopy) and adhesion force measurements with AFM (atomic force microscopy) that oxidative treatment of PS microspheres for long time periods resulted in highly oxidized, low molecular weight fragments on the surface caused by extensive scission of the polymer chain.^{18,19}

Here we have attempted to characterize precisely how the plasma and UVO modification techniques affect the surface properties of the polymers and influence their thermal bonding capabilities. We have used a cyclic olefin polymer (Zeonor[®] 750R) and polystyrene (PS) to study the effect of controlled UV–ozone exposure and oxidative plasma treatment conditions on polymer surface properties. An in-depth characterization of the plasma and UVO modified surfaces is not only beneficial for thermal bonding experiments, but also for other wide-ranging applications, such as protein adsorption and production of surfaces for enhanced cell attachment.^{17,19–21} Zeonor and polystyrene were chosen as the model polymers

for this work because they are extensively used in many different microfluidic applications.^{22–24} The surface modifications of these polymers were studied using XPS, contact angle measurements, AFM roughness measurements, and adhesion force measurements based on AFM force–distance data. We also used the three-point bending experiments to characterize the bond strength of thermally bonded polymer parts and cross-sections of bonded microchannels were analyzed with scanning electron microscopy (SEM) to demonstrate the bonding efficiency of surface-modified polymer substrates.

Experimental

Materials

Cyclic polyolefin resin (Zeonor[®] 750R, T_g 70 °C) was obtained as a gift from Zeon Chemicals (Louisville, KY, USA). Polystyrene resin (STYRON[™] 678C PS, T_g 100 °C, Vicat Softening Point 93.3 °C) was obtained as a gift from Pria Diagnostics (Menlo Park, CA, USA). We used a hot press (Heated Press 4386, Carver, Wabash, IN, USA) to make polymer plaques from the resin. The polymer resins were pressed between two stainless steel plates for 5 min at 500 psi and 100 °C (for Zeonor 750R) and at 120 °C (for PS). After being cooled to room temperature in air, the Zeonor and PS plaques were separated from the stainless steel plates. Radio frequency plasma was generated using room air by an 8–12 MHz plasma cleaner–sterilizer (PDC-32G, Harrick Scientific Corporation, Ossining, NY, USA) at a power of 10.5 W. To generate plasma, room air was allowed to bleed into the plasma cleaner chamber by slightly opening a needle valve on the door of the chamber. Modification times varied from 60 s to 10 min. The UV–ozone treatment was done in a UV–ozone cleaner (BioForce Nanoscience, Ames, IA, USA). The intensity of the mercury grid lamp used was 19.39 mW cm⁻² at a distance of 1.11 cm. The UV lamp had emission wavelengths from 185 to 450 nm (with highest intensity at 253.65 nm) and generated ozone from ambient air within the chamber. The modification times varied from 60 s to 30 min.

Contact angle measurements

Contact angles of distilled water on the modified and unmodified surfaces were measured using a Kruss DSA100 Contact Angle Goniometer (Krüss GmbH, Hamburg, Germany) using the sessile drop method. Contact angles were calculated by the Drop Shape Analysis software using the tangent fit method. Contact angle data was calculated from three different samples and on each sample a minimum of seven different locations were tested.

XPS analysis

The surface chemical composition of treated vs. untreated surfaces was studied by XPS. XPS analyses was performed in a Kratos Axis Ultra (Kratos Analytical, Manchester, UK) spectrometer equipped with a five channel detector and a monochromated aluminium K α X-ray source operating at 150 W with kinetic energy of 1486.6 eV. Survey spectra were obtained with a pass energy of 160 eV and a step size of 1 eV.

Elemental compositions were calculated from the relative intensities of the C 1s and O 1s peak areas obtained from the survey spectra after a linear background subtraction. Further information about the changes in the chemical properties of the surfaces were obtained from the high resolution scans of the C 1s and O 1s regions with a pass energy of 10 eV and a step size of 0.1 eV.

AFM measurements

AFM measurements were performed with a MFP-3D™ microscope (Asylum Research, Santa Barbara, CA, USA). Topographical changes resulting from plasma and UVO treatments were examined and the surface roughness of the samples was calculated in the AC mode with a silicon tip of less than 10 nm diameter and nominal spring constant of 4.5 N m⁻¹. The image analysis and the roughness calculations were carried out with the MFP-3D software. Roughness data was calculated from three different samples and on each sample a minimum of three different regions were imaged.

Force–displacement curves were also obtained with the MFP-3D™ AFM and adhesion force between the AFM tip and the sample was measured. The tip used was the same as for the roughness experiments. Force–displacement curves for treated *vs.* untreated samples were acquired at different temperatures (60 °C, 65 °C and 70 °C for Zeonor 750R and 85 °C, 90 °C and 93 °C for PS) using a heating stage (PolyHeater™, Asylum Research). The polymer samples were attached to magnetic AFM disks with silver paint and the disks were then mounted onto the metal heater stage. The samples were allowed to equilibrate at a certain temperature for 30 min prior to measurement. A force–displacement curve is a plot of the cantilever deflection (an indirect measure of the force) *vs.* the piezo displacement *Z*. To obtain a force–displacement curve, the sample is brought in contact with the AFM tip and then retracted. From the approach contact line of the curve, information about the stiffness of the sample surface can be obtained. During the retraction of the tip, valuable information about the adhesive properties of the sample can be obtained. According to the Johnson–Kendall–Roberts (JKR) theory, a finite negative load is required to separate two surfaces in contact, which is referred to as the pull-off force, and is given by the relation: $F_c = -3\pi R\gamma$, where *R* is the tip radius and γ is the interface energy between the tip and the surface.^{19,20} When the tip is withdrawn from the surface, it does not break contact until the applied force exceeds the tip-surface adhesion force. The adhesion force, F_A , can be measured from the relation: $F_A = -k_c \Delta_C$, where k_c is the spring constant of the tip cantilever and Δ_C is the cantilever deflection under the pull-off force.

Three-point bending tests

The bond strength of the thermally bonded polymer parts were assessed with a three-point bending test in a dynamic mechanical analyzer (Q800 DMA thermal analysis system, TA Instruments, New Castle, DE, USA). For the three-point bend tests, the polymer plaques were cut into rectangular shapes of two different dimensions: 60 mm (L) × 12 mm (W) and 30 mm (L) × 12 mm (W). Two pieces (of separate dimensions)

were then thermally bonded together in the heated press for 2 min at 500 psi and at three different temperatures (60 °C, 65 °C and 70 °C for Zeonor 750R and 85 °C, 90 °C and 93 °C for PS). The untreated and treated samples, bonded at the different temperatures, were then tested at room temperature to examine if the surface treatment conditions and the bonding temperature had any effect on the thermal bonding efficiency of the polymer parts. The load *vs.* displacement curve and the stress *vs.* strain curve of the bonded samples were recorded during the test. Three-point bend testing causes interfacial failure by producing shear stresses at the interface. When the bonded parts start to delaminate, there is a sudden increase in the compliance of the sample, which translates as a sudden drop in the load in the load–displacement curve. The maximum stress (from the stress *vs.* strain curve) that the bonded sample can uphold prior to delamination was used to characterize the bonding efficiency of the samples at the different temperatures.

Microchannel cross-sections

The microchannels were fabricated by hot-embossing with an SU-8 mold in a heated press. The fabrication process is described elsewhere.²² The microchannels were then cross-sectioned using an IsoMet® Low Speed Saw (Buehler Ltd., Lake Bluff, IL, USA) and a precision diamond tipped cutting blade. The sections were imaged using SEM (SUPRA 40VP, Carl Zeiss Inc, Germany) to characterize the dimensions of the microchannels after the bonding process.

Results and discussion

XPS analysis

The XPS data indicate that the polymer samples treated by plasma and UVO consistently incorporated oxygen into the surface layer. Fig. 2 shows % oxygen incorporation relative to total oxygen and carbon for different treatment times and conditions as measured by XPS. Unmodified Zeonor contains an average of 3.15% oxygen, which increased to about 27% after 10 min of plasma treatment and to about 14% after 10 min of UVO treatment. Unmodified polystyrene contains an average of 1.4% oxygen, which increased to about 24% and 35% after 10 min of plasma and UVO treatment respectively. Rinsing the samples in millipore water after the treatments effectively removed some of the surface oxygen, suggesting that some low-molecular weight species and oxidized debris may have been removed from the surface *via* washing. The oxygen level reduced to 22% after rinsing for plasma treated Zeonor. For polystyrene, the oxygen levels dropped from 24% to 16% for plasma treated samples and for UVO treated samples the level dropped from 35% to 25% after rinsing. However, in case of UVO treated Zeonor, the level of oxygen unexpectedly increased from 14% to 19% after rinsing. It appears that samples with comparatively low modification levels (less than ~15% oxygen) were relatively stable in water and there could possibly have been a small amount of oxygen uptake from the residual H₂O following rinsing. High resolution C 1s XPS spectra show the nature of the surface chemical groups produced by the plasma and UVO modifications

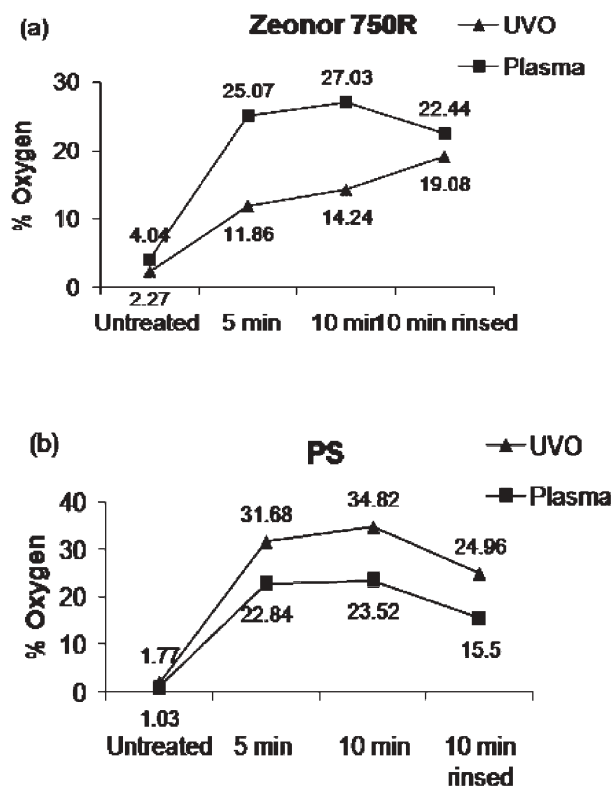


Fig. 2 Percent surface oxygen measured by XPS for plasma and UVO treated (a) Zeonor 750R, (b) polystyrene.

(Fig. S1 and Fig. S2 in the ESI†). All of the C 1s spectra have been calibrated to fit the peak maximum at 285 eV. As seen in the Figures, the surface modifications produced chemical groups at higher binding energies, which were not present in the native samples. These chemical groups may be attributed to oxygen-containing species, such as C—O, C=O, O—C=O, created due to extensive scission of the polymer chain and oxidative reactions on the surface, resulting in an increase in the surface oxygen concentration. The O 1s spectra of the treated surfaces were relatively broad with only one obvious peak indicating multiple types of oxygen bonding.

Contact angle measurements

Contact angles of distilled water on Zeonor and PS surfaces were measured to examine the wettability of the surfaces after the treatments by plasma and UV–ozone. Fig. 3 shows the contact angle on treated Zeonor and PS as a function of treatment time ($n = 3$). In case of UVO treatment, the value of contact angle decreased rapidly from 95° to about 52° for Zeonor and from 85° to about 19° for polystyrene and reached saturation after 10 min of treatment. With plasma modification, the contact angle values dropped steadily to <5° after 10 min of treatment and no saturation effect was observed. The drop in contact angle is believed to be due to the incorporation of polar, oxygen-containing functional groups into the surface layer, resulting in higher surface free energy. The increase in wettability is concomitant with the increase in surface oxygen concentration as shown by the XPS data, although the two phenomena are not exclusively related.

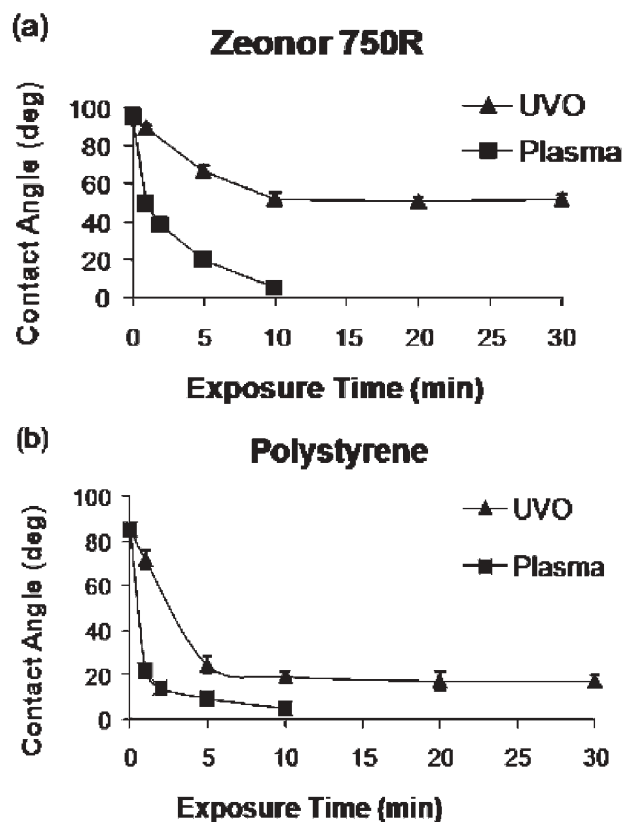


Fig. 3 Contact angles of plasma and UVO treated (a) Zeonor 750R, (b) polystyrene.

Contact angle results are also influenced by surface disorders and high surface roughness tends to increase contact angle values.²⁵ In the case of polystyrene, we observed that UVO treatment resulted in a higher concentration of surface oxygen, although the drop in contact angle was greater with plasma treatment. This could possibly be due to the greater increase in surface roughness, resulting from UVO treatment as compared to plasma treatment (discussed in the next section) which can lead to an increase in contact angle values on UVO treated samples.

AFM measurements

Fig. 4 shows representative AFM images of Zeonor and PS surfaces before and after 10 min of plasma and UVO treatments. The surfaces became visibly rougher following modification and the RMS roughness values increased significantly. The increased roughness is attributed to plasma or UVO induced scission of the polymer chains and local melting on the surfaces.

AFM force–distance curves were also acquired for the treated and untreated surfaces at different temperatures. AFM has the capability of performing local measurements with vertical resolution in the sub-nanometre range. This resolution gives the opportunity to characterize sample properties (such as stiffness, adhesion force *etc.*) and to determine T_g differences in the very surface layer of the sample which is modified by the treatment conditions.^{18,26} Force–distance

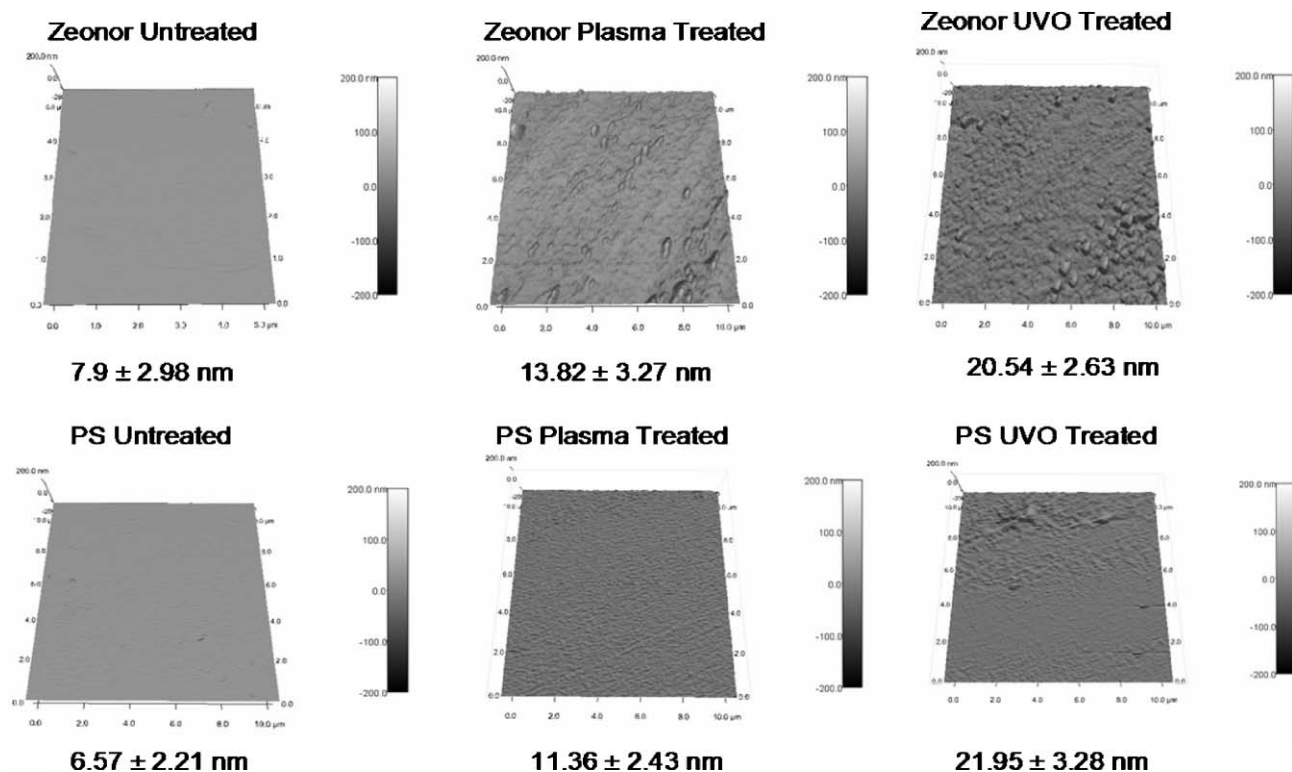


Fig. 4 AFM images of native and surface treated Zeonor 750R and polystyrene sample.

curves measured between the surface and the AFM tip are shown in Fig. S3 in the ESI†. There is an increase in pull-off force with treatment, indicating an increase in adhesion between the tip and the sample surface. There is also an increase in adhesion force with increasing temperature. From the decrease in the slope of the contact line of the force–distance curves, it can be observed that the stiffness of the surface decreases with treatment. The stiffness of the sample was quantified by taking the first derivative of the approach contact line. This method can yield qualitative information about changes in surface stiffness, but is not necessarily the best method to obtain quantitative values of surface modulus. The calculated adhesion forces between the tip and the surface and the stiffness of the surface are shown in Fig. 5 ($n = 3$).

The increase in surface adhesion force and the decrease in stiffness of the surface are attributed to the presence of high surface energy, low molecular weight, oxygen-containing functional groups on the surface (as found with the XPS data). The drop in stiffness and increase in adhesion force indicate a depression of the glass transition at the polymer surface.^{27,28} The T_g of the bulk polymer is believed to be unchanged since the modification techniques involve only the surface of the polymer.

The XPS, contact angle and AFM data all suggest that the plasma and UVO treatments result in the production of low molecular weight polymer fragments, with oxygen-containing chemical groups on the surface through chain scission and oxidative reactions, which imply a corresponding drop in the glass transition temperature at the surface.²⁹ The next step in this work was to investigate if it is possible to thermally bond two surface-treated polymer pieces at a temperature below the

T_g of the material. The rationale is that if the surface T_g is lowered, it will be possible for the surface layers of the plastic pieces to flow and fuse with each other at a temperature lower than the T_g of the bulk polymer. The bonding strength of the sealed polymer pieces was then tested with DMA three-point bending tests.

Three-point bending test

As seen in the load–displacement curves in Fig. S4 in the ESI†, the samples sealed at a higher temperature de-bonded at a higher applied load. However, if the samples were pretreated with plasma or UVO, the bond strength of the samples increased, even when they were bonded at comparatively lower temperatures. The maximum stress on the bonded samples prior to de-bonding (‘stress at failure’) was calculated from the stress–strain plots of the three-point bend tests. Fig. 6 shows the stress at failure of the bonded samples ($n = 6$ for Zeonor 750R samples and $n = 4$ for PS samples). As seen in the Figure, the stress at failure of plasma and UVO treated Zeonor surfaces bonded at 65 °C is higher than that of untreated samples bonded at 70 °C (T_g). Similar results were observed for polystyrene as well, with slightly better performance of UVO treated samples in comparison to plasma treated samples. The maximum stress on the plasma and UVO treated polystyrene surfaces bonded at 90 °C is higher than that on untreated samples bonded at 93 °C (Vicat softening point of PS). The DMA three-point bending test results demonstrate that the thermal bonding efficiencies of the polymeric materials were enhanced after plasma and UVO treatments and successful bonding was achieved between two plastic

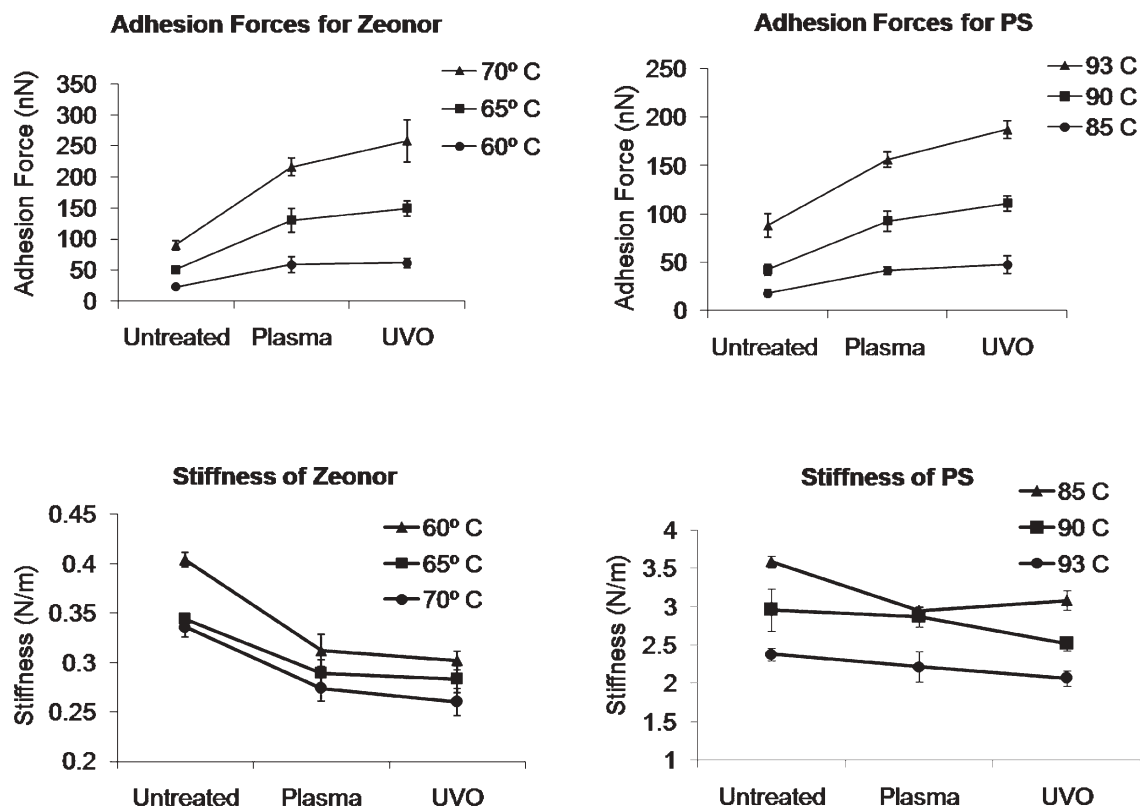


Fig. 5 Surface adhesion force and surface stiffness obtained from AFM at different temperatures and treatment conditions.

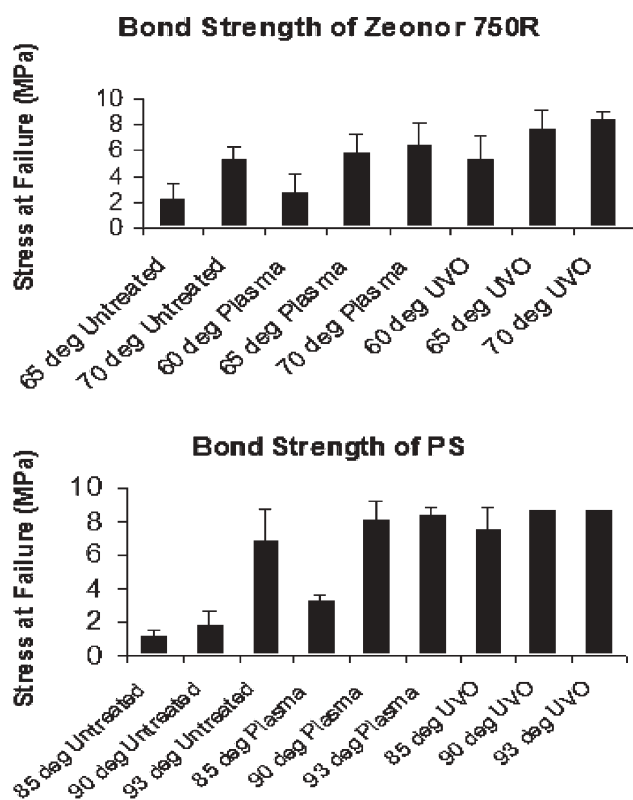


Fig. 6 Maximum stress on the bonded Zeonor 750R and PS samples prior to delamination.

pieces at temperatures substantially below the T_g or the Vicat softening temperature of the polymer.

Cross-sections of microchannels

Fig. 7 shows the cross-section images of the microchannels bonded after plasma and UVO treatment. The pretreated Zeonor samples were bonded at 65 °C and the polystyrene samples were bonded at 90 °C. As seen in the Figures, the microchannels bonded at lower temperatures were not deformed and maintained a tight seal with the cover plate.

Conclusions

The effect of plasma and UVO treatments on the surface properties of Zeonor 750R and PS was investigated with

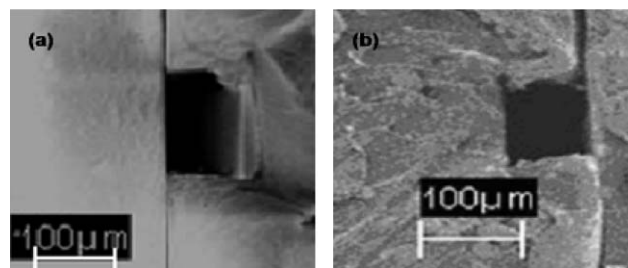


Fig. 7 SEM micrographs of (a) cross-section of Zeonor channels bonded at 65 °C after plasma treatment, (b) cross-section of PS channel bonded at 90 °C after UVO treatment.

reference to their thermal bonding capabilities. The surface chemical properties were characterized with XPS and contact angle measurements. The XPS data indicated an increase in surface oxygen content and concomitant increase in C 1s binding energies as a result of the surface modifications. This was accompanied by a decrease in the measured contact angles of the modified surfaces. AFM data shows that the surface roughness increases as a result of the exposure to UV-ozone and oxygen plasma. The adhesion forces between the tip and the sample also increases due to the treatments and there is a drop in the stiffness of the modified samples, which suggests a corresponding drop in the surface glass transition. The physicochemical modifications also result in improved wetting of the surfaces with high surface free energy and can lead to better electrostatic interactions between the joining surfaces, which may also contribute towards improved bonding coupled with the reduced T_g . The bond strength of thermally bonded polymer parts was assessed using the DMA in the three-point bending mode to observe the delamination of two bonded parts. The DMA results show a significant increase in the bond strength of the parts sealed at a temperature below the T_g after UVO and plasma treatments. The dimensions of the microchannels also remained intact when the thermal bonding was done at temperatures below the glass transition temperature of the polymer. The results demonstrate that plasma and UVO surface modifications are effective treatments for improving the thermal bonding efficiency of polymeric microfluidic devices.

References

- 1 R. M. McCormick, R. J. Nelson, M. G. Alonso-Amigo, D. J. Benvegnu and H. H. Hooper, *Anal. Chem.*, 1997, **69**, 2626.
- 2 J. Liu, T. Pan, A. T. Woolley and M. L. Lee, *Anal. Chem.*, 2004, **76**, 6948.
- 3 J. Yakovleva, R. Davidsson, M. Bengtsson, T. Laurell and J. Emnéus, *Biosens. Bioelectron.*, 2003, **19**, 21.
- 4 L. Zhu and S. A. Soper, *Anal. Biochem.*, 2004, **330**, 206.
- 5 S. M. Ford, B. Kar, S. McWhorter, J. Davies, S. A. Soper, M. Klopff, G. Calderon and V. Saile, *J. Microcolumn Sep.*, 1998, **10**, 413.
- 6 M. B. Esch, S. Kapur, G. Irizarry and V. Genova, *Lab Chip*, 2003, **3**, 121.
- 7 L. Martynova, L. E. Locascio, M. Gaitan, G. W. Kramer, R. G. Christensen and W. A. MacCrehan, *Anal. Chem.*, 1997, **69**, 4783.
- 8 M. A. Roberts, J. S. Rossier, P. Bercier and H. Girault, *Anal. Chem.*, 1997, **69**, 2035.
- 9 R. T. Kelly and A. T. Woolley, *Anal. Chem.*, 2003, **75**, 1941.
- 10 Z. Chen, Y. Gao, J. Lin, R. Su and Y. Xie, *J. Chromatogr., A*, 2004, **1038**, 239.
- 11 L. G. Song, D. F. Fang, R. K. Kobos, S. J. Pace and B. Chu, *Electrophoresis*, 1999, **20**, 2847.
- 12 J. D. Xu, L. Locascio, M. Gaitan and C. S. Lee, *Anal. Chem.*, 2000, **72**, 1930.
- 13 A. Muck, Jr., J. Wang, M. Jacobs, G. Chen, M. P. Chatrathi, V. Jurka, Z. Výborný, S. D. Spillman, G. Sridharan and M. J. Schöning, *Anal. Chem.*, 2004, **76**, 2290.
- 14 L. E. Locascio, C. E. Perso and C. S. Lee, *J. Chromatogr., A*, 1999, **857**, 275.
- 15 Z. Wu, N. Xanthopoulos, F. Reymond, J. S. Rossier and H. H. Girault, *Electrophoresis*, 2002, **23**, 782.
- 16 R. Truckenmüller, P. Henzi, D. Herrmann, V. Saile and W. K. Schomburg, *Microsyst. Technol.*, 2004, **10**, 372.
- 17 B. W. Callen, M. L. Ridge, S. Lahooti, A. W. Neumann and R. N. S. Sodhi, *J. Vac. Sci. Technol., A*, 1995, **13**, 2023.
- 18 G. V. Lubarsky, M. R. Davidson and R. H. Bradley, *Surf. Sci.*, 2004, **558**, 135.
- 19 G. V. Lubarsky, M. R. Davidson and R. H. Bradley, *Appl. Surf. Sci.*, 2004, **227**, 268.
- 20 D. O. H. Teare, N. Emmison, C. Ton-That and R. H. Bradley, *Langmuir*, 2000, **16**, 2818.
- 21 A. S. G. Curtis, J. V. Forrester, C. McInnes and F. Lawrie, *J. Cell Biol.*, 1983, **97**, 1500.
- 22 A. Bhattacharyya and C. M. Klapperich, *Anal. Chem.*, 2006, **78**, 788.
- 23 J. Kameoka, H. G. Craighead, Z. Hongwei and J. Henion, *Anal. Chem.*, 2001, **73**, 1935.
- 24 M. Pribyl, D. Snita and M. Marek, *Technical Proceedings of the NSTI Nanotechnology Conference and Trade Show*, Anaheim, CA, USA, 2005, vol. 1, p. 672.
- 25 T. K. Murakami, Y. Fukushima, Y. Hirano, Y. Tokuoka, M. Takahashi and N. Kawashima, *Colloids Surf., B*, 2003, **29**, 171.
- 26 R. C. Chatelier, X. Xie, T. R. Gengenbach and H. J. Griesser, *Langmuir*, 1995, **11**, 2585.
- 27 D. H. Gracias, D. Zhang, L. Lianos, W. Ibach, Y. R. Shen and G. A. Somorjai, *Chem. Phys.*, 1999, **245**, 277.
- 28 S. Ge, Y. Pu, W. Zhang, M. Rafailovich, J. Sokolov, C. Buenviaje, R. Buckmaster and R. M. Overney, *Phys. Rev. Lett.*, 2000, **85**, 2340.
- 29 H. Fischer, *Macromolecules*, 2005, **38**, 844.